On the importance of meanflow propagation effects for jet noise modelling

Sergey Karabasov

UNIVERSITY OF CAMBRIDGE

ИБРАЭ

CELEBRATE 350 YEARS

THE ROYAL SOCIETY

Plan

- Background
- Goldstein acoustic analogy informed by LES
- Numerical testing
- Discussion

Background

- In the last two decades, most of the jet noise reduction for civil aircraft came from increasing the size of jet engines. This allowed engineers to reduce the jet speed for the same amount of thrust and, since jet noise scales as a high power of the jet exit velocity, in accordance with the Lighthill v^8 law, this reduces the noise.

$$\left(\frac{1}{{c_0}^2}\frac{\partial^2}{\partial t^2}-\frac{\partial^2}{\partial x_i \partial x_i}\right)(\rho-\rho_0)=q(\mathbf{x},t),$$

$$p(\mathbf{x},t)=\frac{1}{4\pi}\frac{\partial^2}{\partial x_i \partial x_j}\int\frac{1}{|\mathbf{x}-\mathbf{y}|}T_{ij}\left(\mathbf{y},t-\tau-\frac{|\mathbf{x}-\mathbf{y}|}{c_0}\right)d^3\mathbf{y},$$

$$q(\mathbf{x},t)=\frac{\partial^2}{\partial x_i \partial x_j}\left(\rho v_i v_j+((p-p_0)-{c_0}^2(\rho-\rho_0))\delta_{ij}-\sigma_{ij}\right)=\frac{\partial^2}{\partial x_i \partial x_j}T_{ij}$$

- Lighthill: Power~ $l^{-1}\rho v^3 M^5 V_0$

Background

- In the last two decades, most of the jet noise reduction for civil aircraft came from increasing the size of jet engines. This allowed engineers to reduce the jet speed for the same amount of thrust and, since jet noise scales as a high power of the jet exit velocity, in accordance with the Lighthill v^8 law, this reduces the noise.

$$\left(\frac{1}{{c_0}^2}\frac{\partial^2}{\partial t^2}-\frac{\partial^2}{\partial x_i \partial x_i}\right)(\rho-\rho_0)=q(\mathbf{x},t),$$

$$p(\mathbf{x},t)=\frac{1}{4\pi}\frac{\partial^2}{\partial x_i \partial x_j}\int\frac{1}{|\mathbf{x}-\mathbf{y}|}T_{ij}\left(\mathbf{y},t-\tau-\frac{|\mathbf{x}-\mathbf{y}|}{c_0}\right)d^3\mathbf{y},$$

$$q(\mathbf{x},t)=\frac{\partial^2}{\partial x_i \partial x_j}\left(\rho v_i v_j+((p-p_0)-{c_0}^2(\rho-\rho_0))\delta_{ij}-\sigma_{ij}\right)=\frac{\partial^2}{\partial x_i \partial x_j}T_{ij}$$

- Lighthill: Power~ $l^{-1}\rho v^3 M^5 V_0$
- But for further jet noise reduction, the detailed mechanisms of turbulent jet noise need to be quantified

The role of sound interference effects within the distributed source

- Michel (AIAA 2007,2009)
- Used the Michalke source model and included sound interference effects

The role of sound interference effects within the distributed source

- Michel (AIAA 2007,2009)
- Used the Michalke source model and included sound interference effects
- Can explain many important jet noise effects

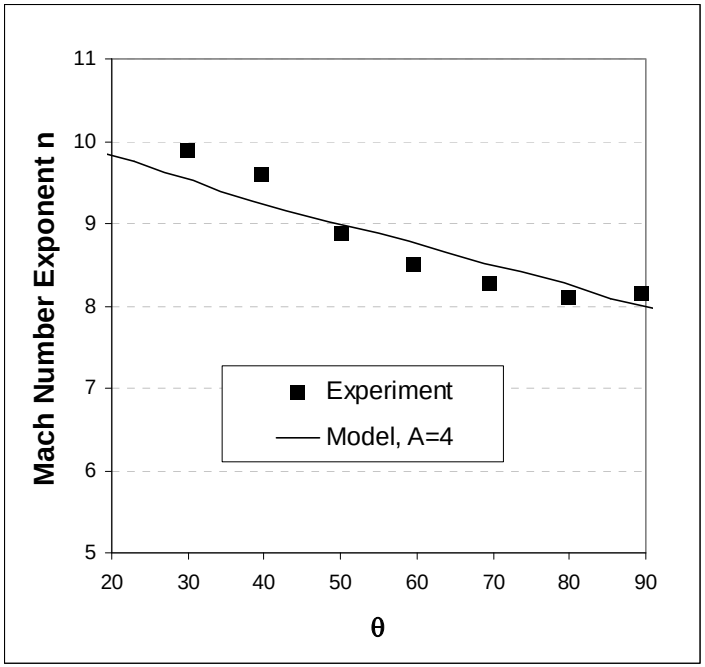

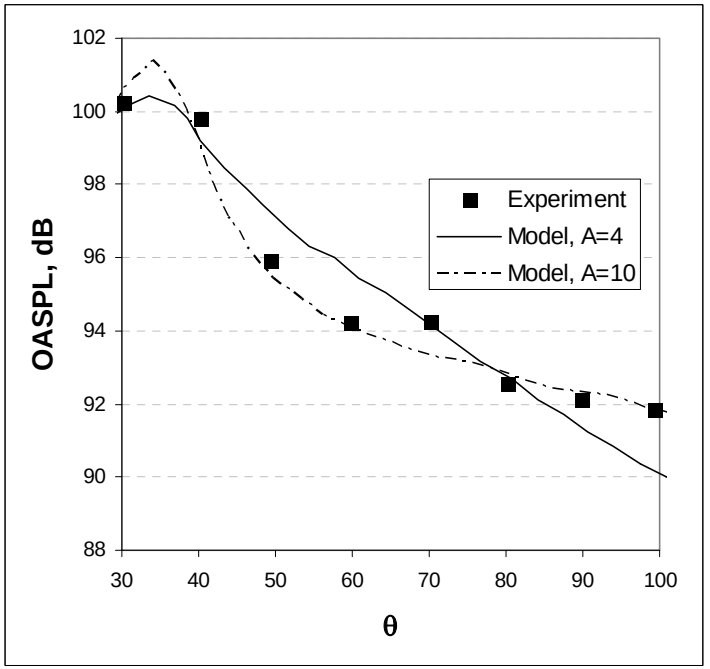

The role of sound interference effects within the distributed source

- Michel (AIAA 2007,2009)
- Used the Michalke source model and included sound interference effects
- Can explain many important jet noise effects (but not the spectra!)

Important parameters $f, L_x = \int_{-\infty}^{+\infty} \gamma_q(\Delta_1) d\Delta_1$ and v_p Best agreement for $f \cdot L_x \sim v_p \sim c_0$

Suggests that large structures can seen as small scales, depends on *f*

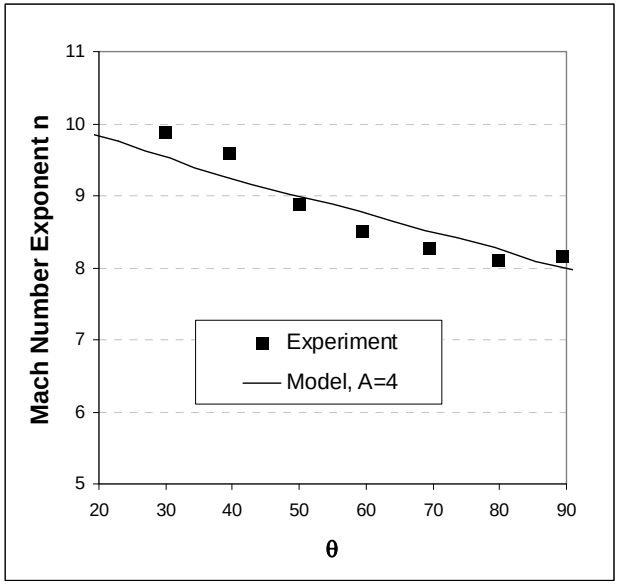

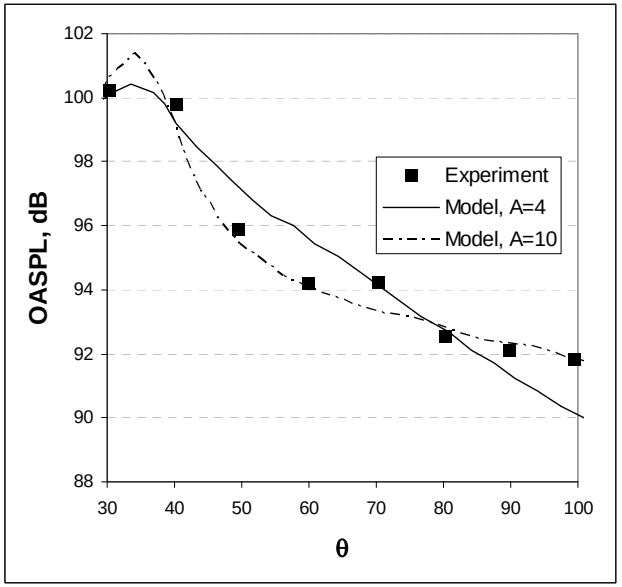

Acoustic Analogy informed by LES

M.Afsar, SK, T.Hynes, A.Dowling, J.McGuirk, G.Page

- Use the Goldstein (2003) decomposition

$$\frac{\partial \rho'}{\partial \tau} + \frac{\partial}{\partial y_j}(\rho' \tilde{v}_j + u_j) = 0$$

$$\frac{\partial u_i}{\partial \tau} + \frac{\partial}{\partial y_j}(\tilde{v}_j u_i) + \frac{\partial p'}{\partial y_i} + u_j \frac{\partial \tilde{v}_i}{\partial y_j} - \left(\frac{\rho'}{\bar{\rho}}\right)\frac{\partial \tilde{\tau}_{ij}}{\partial y_j} = \frac{\partial T'_{ij}}{\partial y_j} \quad i = 1,..3.$$

$$\left(\frac{1}{\gamma - 1}\right)\frac{\partial p'}{\partial \tau} + \left(\frac{1}{\gamma - 1}\right)\frac{\partial}{\partial y_j}(p' \tilde{v}_j) + \frac{\partial}{\partial y_j}(u_j \tilde{h}) + p' \frac{\partial \tilde{v}_j}{\partial y_j} - \left(\frac{u_i}{\bar{\rho}}\right)\frac{\partial \tilde{\tau}_{ij}}{\partial y_j} = Q.$$

Acoustic Analogy informed by LES

M.Afsar, SK, T.Hynes, A.Dowling, J.McGuirk, G.Page

- Use the Goldstein (2003) decomposition

$$\frac{\partial \rho'}{\partial \tau} + \frac{\partial}{\partial y_j}(\rho' \tilde{v}_j + u_j) = 0$$

$$\frac{\partial u_i}{\partial \tau} + \frac{\partial}{\partial y_j}(\tilde{v}_j u_i) + \frac{\partial p'}{\partial y_i} + u_j \frac{\partial \tilde{v}_i}{\partial y_j} - \left(\frac{\rho'}{\bar{\rho}}\right)\frac{\partial \tilde{\tau}_{ij}}{\partial y_j} = \frac{\partial T'_{ij}}{\partial y_j} \quad i = 1,..3.$$

$$\left(\frac{1}{\gamma - 1}\right)\frac{\partial p'}{\partial \tau} + \left(\frac{1}{\gamma - 1}\right)\frac{\partial}{\partial y_j}(p' \tilde{v}_j) + \frac{\partial}{\partial y_j}(u_j \tilde{h}) + p' \frac{\partial \tilde{v}_j}{\partial y_j} - \left(\frac{u_i}{\bar{\rho}}\right)\frac{\partial \tilde{\tau}_{ij}}{\partial y_j} = Q.$$

- The power spectral density integral is obtained as a convolution of the source term with the propagator function

$$P(\mathbf{x}, \omega) = \int_{V_\infty(\mathbf{y})} \int_{Д} R_{ijkl}(\mathbf{y}, Д, \omega) I_{ij}(\mathbf{y}, \omega \mid \mathbf{x}) I_{kl}(\mathbf{y} + Д, -\omega \mid \mathbf{x})\, d^3 Д\, d^3 \mathbf{y}$$

- where

$$R_{ijkl}(\mathbf{y}, Д, \tau) = \overline{\rho(\mathbf{y} + Д, t + \tau) v_i''(\mathbf{y} + Д, t + \tau) v_j''(\mathbf{y} + Д, t + \tau) \rho(\mathbf{y}, t) v_k''(\mathbf{y}, t) v_l''(\mathbf{y}, t)} -$$
$$\overline{\rho(\mathbf{y} + Д, t + \tau) v_i''(\mathbf{y} + Д, t + \tau) v_j''(\mathbf{y} + Д, t + \tau)} \cdot \overline{\rho(\mathbf{y}, t) v_k''(\mathbf{y}, t) v_l''(\mathbf{y}, t)}$$

Two-point two-time velocity correlations

- The non-dimensional shapes of the 4th order 2-point 2-time correlations of the turbulent Reynolds stresses R_{ijkl} are determined by fitting

$$R_{ijkl}(\mathbf{y}, Д, \tau) = A_{ijkl}(\mathbf{y}) \exp[-\Delta_1 / (\tilde{v}_1 \cdot \tau_s(\mathbf{y})) - \ell n 2\left((\Delta_1 - \tilde{v}_1 \cdot \tau)^2 + \Delta_2^2 + \Delta_3^2\right) / l_s^2(\mathbf{y})].$$

to LES predicted correlations

Good comparison of the JEAN LES correlation coefficients with the experiments

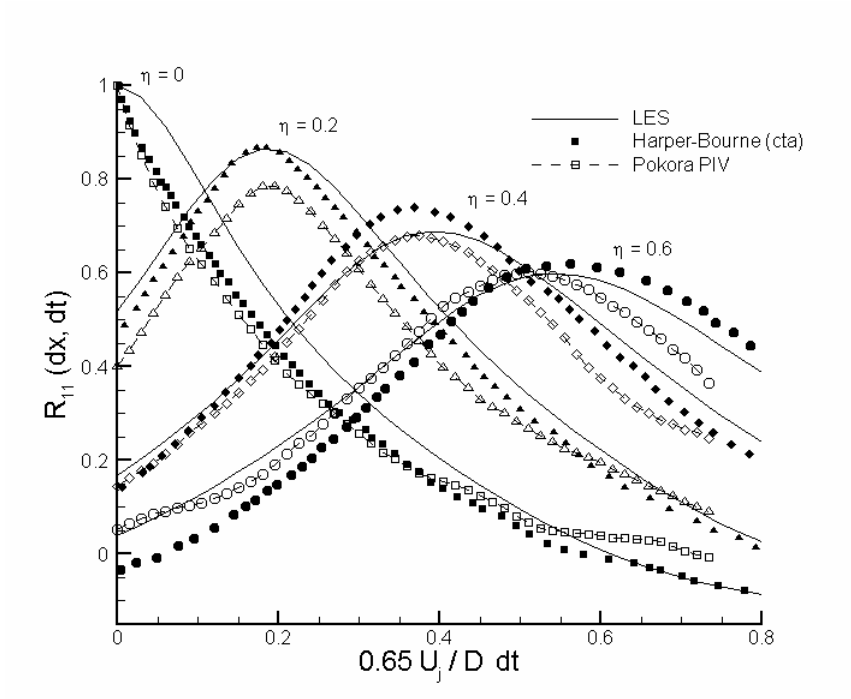

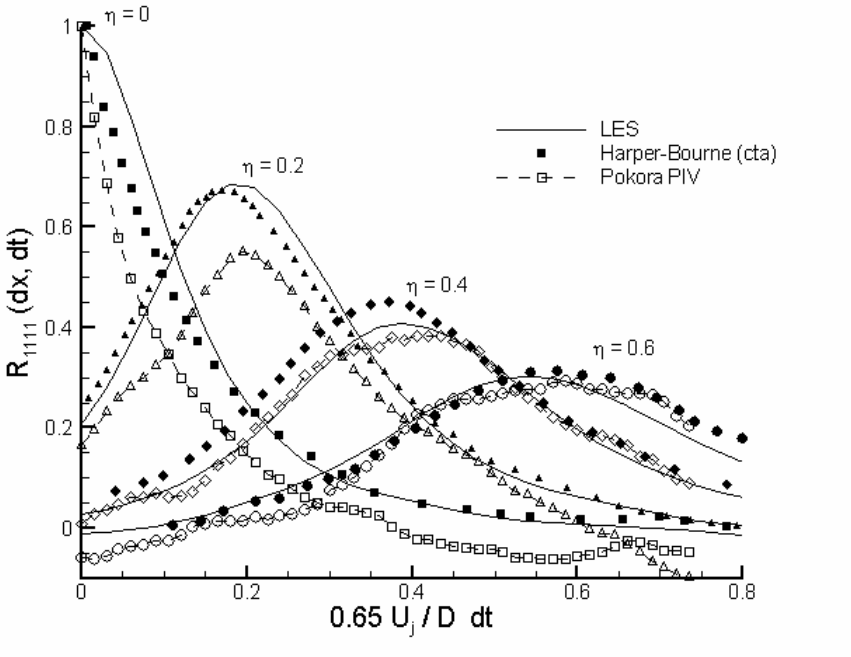

Two-point two-time velocity correlations

- The non-dimensional shapes of the 4th order 2-point 2-time correlations of the turbulent Reynolds stresses R_{ijkl} are determined by fitting

$$R_{ijkl}(\mathbf{y}, Д, \tau) = A_{ijkl}(\mathbf{y}) \exp[-\Delta_1 / (\tilde{v}_1 \cdot \tau_s(\mathbf{y})) - \ell n 2\left((\Delta_1 - \tilde{v}_1 \cdot \tau)^2 + \Delta_2^2 + \Delta_3^2\right) / l_s^2(\mathbf{y})].$$

to LES predicted correlations

- The time and length scales used in the non-dimensional R_{ijkl} can be taken to be proportional to the length and time scales at that position obtained from a RANS calculation. **NO empirical fitting to the far-field sound!**
- In principle, the reconstruction can be done avoiding the RANS step, e.g., if the high-resolution LES data are available in several 2D cut-planes through the jet (could be difficult to obtain well-converged data for all jet locations)

Solving Linearised Euler equations

System of (direct) linearised Euler equations

$$\mathbf{L}\cdot\mathbf{V}^{(n)} = Sources(\mathbf{y}),\ p(\mathbf{x}) = \int_{R^3} G(\mathbf{x}|\mathbf{y})Sources(\mathbf{y})dy,$$

$$\mathbf{V}^{(n)T} = (\rho, u, v, w, p), \mathbf{x} = farfield, \mathbf{y} = nearfield$$

Avoiding having to compute Green's function at every point of the source volume: Use the Representation Theorem

$$p(\mathbf{x}) = \int_{R^3} \mathbf{G}^T \cdot \left(\mathbf{L}\cdot\mathbf{V}^{(n)}\right)\cdot d^3\mathbf{y} = \int_{R^3} \mathbf{L}\cdot\left(\mathbf{G}^T\cdot\mathbf{V}^{(n)}\right)\cdot d^3\mathbf{y} + \int_{R^3} \mathbf{V}^{(n)T}\cdot\left(\mathbf{L}^*\cdot\mathbf{G}^*\right)\cdot d^3\mathbf{y} = \int_{R^3} \mathbf{V}^{(n)T}\cdot\left(\mathbf{L}^*\cdot\mathbf{G}^*\right)\cdot d^3\mathbf{y},$$

$$(\int_{R^3} \mathbf{L}\cdot\left(\mathbf{G}^T\cdot\mathbf{V}^{(n)}\right)\cdot d^3\mathbf{y} = 0)$$

$$\int_{R^3} \mathbf{V}^{(n)T}\cdot\left(\mathbf{L}^*\cdot\mathbf{G}^*\right)\cdot d^3\mathbf{y} = \int_{R^3} \mathbf{V}^{(n)T}\cdot(0,0,0,\delta(\mathbf{y}-\mathbf{x}))^T\cdot d^3\mathbf{y} = p(\mathbf{x}).$$

Solving Linearised Euler equations

System of (direct) linearised Euler equations

$$\mathbf{L}\cdot\mathbf{V}^{(n)} = Sources(\mathbf{y}),\ p(\mathbf{x}) = \int_{R^3} G(\mathbf{x}|\mathbf{y})Sources(\mathbf{y})dy,$$

$$\mathbf{V}^{(n)T} = (\rho, u, v, w, p), \mathbf{x} = farfield, \mathbf{y} = nearfield$$

Avoiding having to compute Green's function at every point of the source volume: Use the Representation Theorem

$$p(\mathbf{x}) = \int_{R^3} \mathbf{G}^T \cdot \left(\mathbf{L}\cdot\mathbf{V}^{(n)}\right)\cdot d^3\mathbf{y} = \int_{R^3} \mathbf{L}\cdot\left(\mathbf{G}^T\cdot\mathbf{V}^{(n)}\right)\cdot d^3\mathbf{y} + \int_{R^3} \mathbf{V}^{(n)T}\cdot\left(\mathbf{L}^*\cdot\mathbf{G}^*\right)\cdot d^3\mathbf{y} = \int_{R^3} \mathbf{V}^{(n)T}\cdot\left(\mathbf{L}^*\cdot\mathbf{G}^*\right)\cdot d^3\mathbf{y},$$

$$\left(\int_{R^3} \mathbf{L}\cdot\left(\mathbf{G}^T\cdot\mathbf{V}^{(n)}\right)\cdot d^3\mathbf{y} = 0\right)$$

$$\int_{R^3} \mathbf{V}^{(n)T}\cdot\left(\mathbf{L}^*\cdot\mathbf{G}^*\right)\cdot d^3\mathbf{y} = \int_{R^3} \mathbf{V}^{(n)T}\cdot(0,0,0,\delta(\mathbf{y}-\mathbf{x}))^T\cdot d^3\mathbf{y} = p(\mathbf{x}).$$

From which the adjoint Green's function is determined by numerically solving:

$$\mathbf{L}^*\cdot\mathbf{G}^* = (0,0,0,\delta(\mathbf{y}-\mathbf{x}))^T$$

Spurious linear instability waves are suppressed!

Summary of the results

- In many points of the jet the correlation coefficients adhere to the prescribed analytical form well

x/D=2

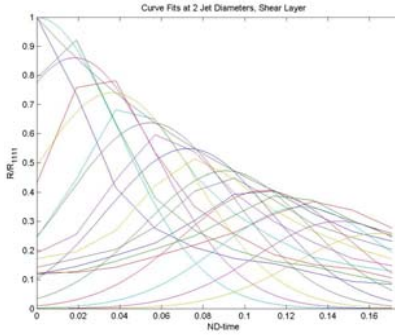

x/D=6

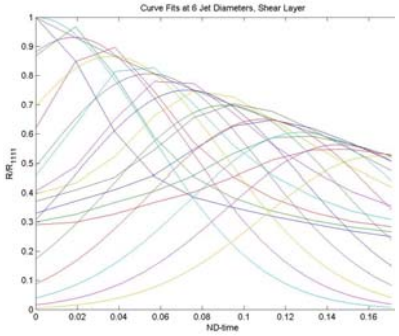

- Only several of Rijkl are important to retain in the model

Summary of the results

- In many points of the jet the correlation coefficients adhere to the prescribed analytical form well

x/D=2

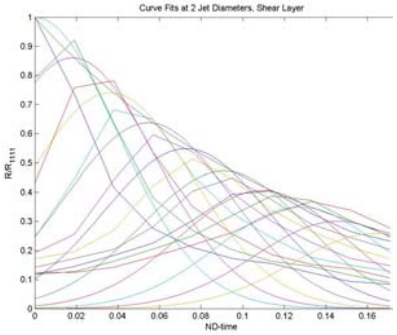

x/D=6

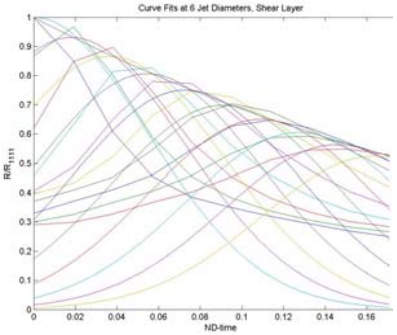

- Only several of Rijkl are important to retain in the model
- In the frequency domain the adjoint Green's function equations can be efficiently solved avoiding the numerical instability problem

LES data from H.Xia, P.Tucker

Encouraging agreement with the experiment (2-2.5dB)

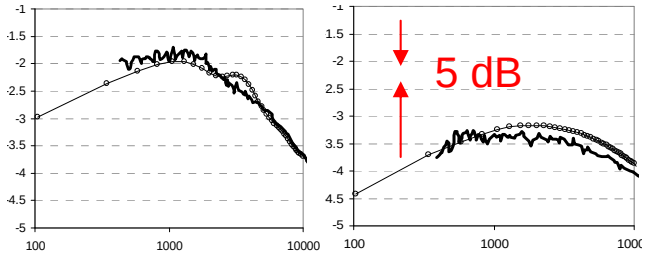

JEAN case

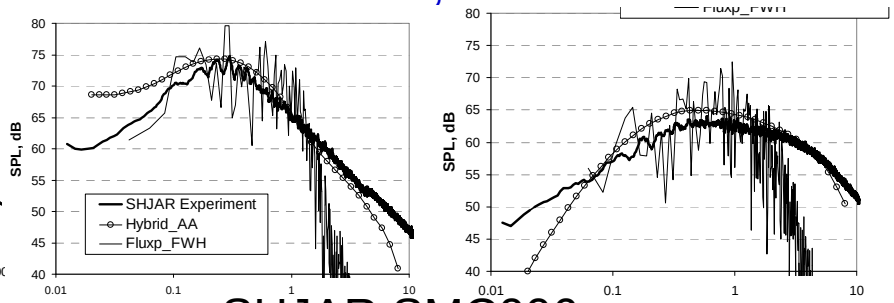

SHJAR SMC006 case

Jet noise spectra directivity

- Michalke and Fuchs (1975), Laufer et al (1976), Michalke (1977), Moore (1977), Tam et al (e.g.,1984, 1996, 2008)

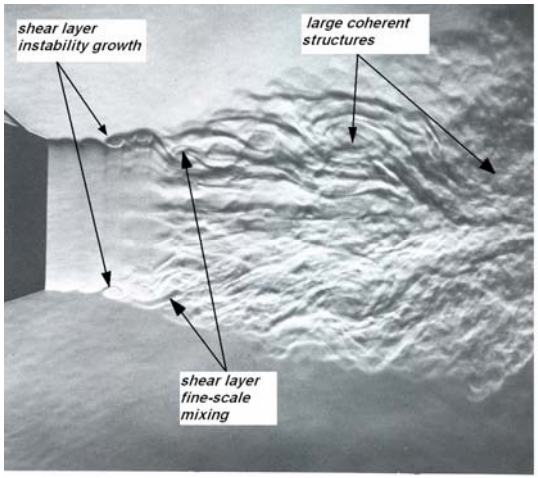

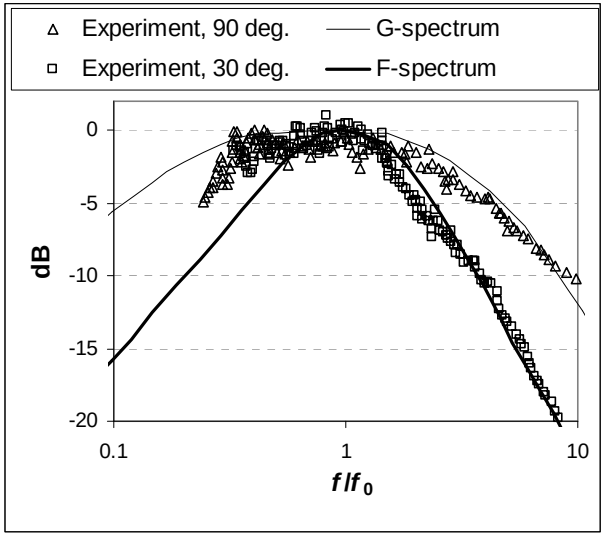

- The Fine Scale Spectra – Large Scale Spectra: Self-similar G- and F- Spectra can be used as a universal tool to check the consistency of the experimental data (e.g., Viswanathan 2004)

Our model allows to check the effect of propagation model on the spectra shape

Following Tam et al (2008), normalise the spreading jet solution by amplitude and peak frequency f_0 and compare with the FSS-LSS spectra

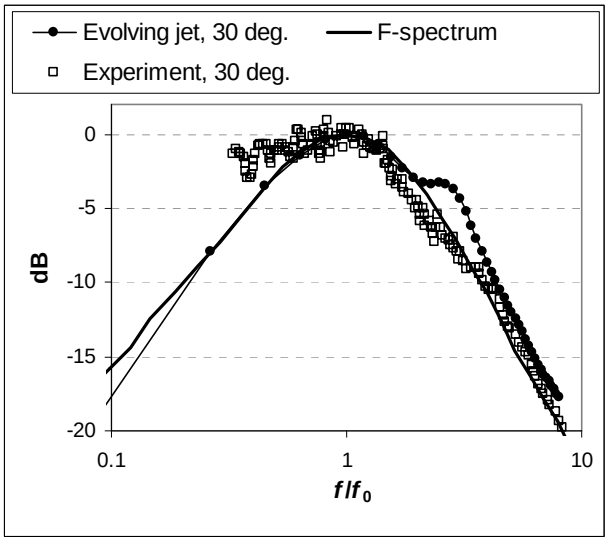

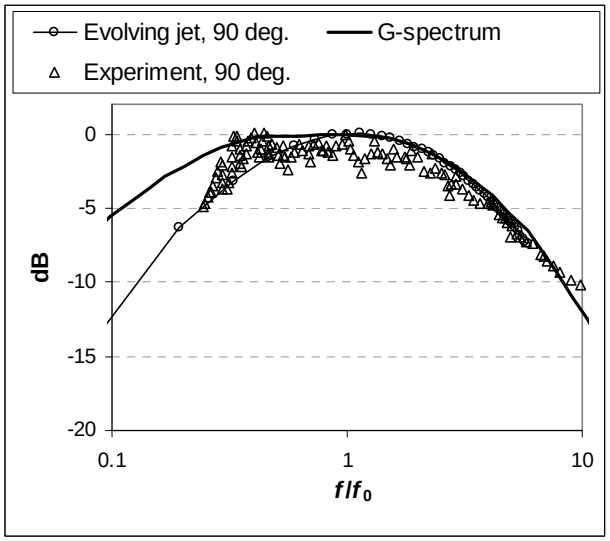

Good agreement with both universal spectral shapes (within 2dB)

Our model allows to check the effect of propagation model on the spectra shape

Karabasov et al, AIAA J 2010; Karabasov PhilTransA 2010

Following Tam et al (2008), normalise the locally parallel jet solution by amplitude and peak frequency f_0 and compare with the FSS-LSS spectra

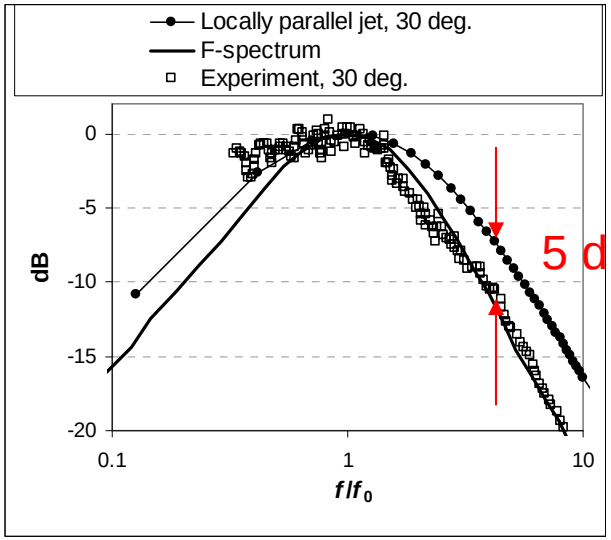

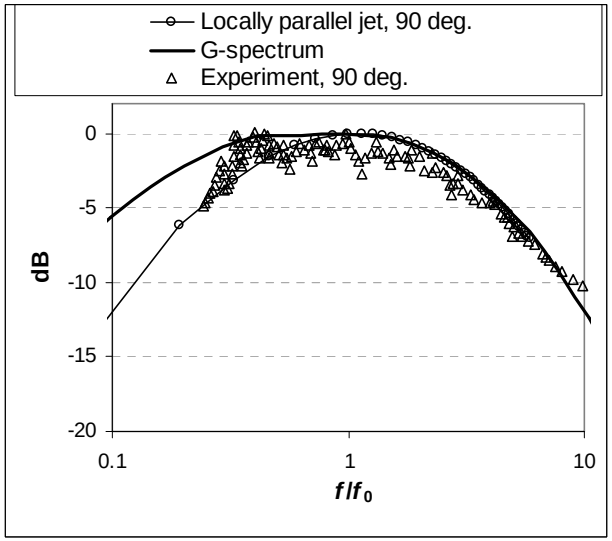

Doesn't capture the correct shape for the 30^0 to the jet

The effect of sound propagation can be also investigated for idealised ring sources
Upto 4D errors in apparent source location if a wrong propagation model is used!

Can the effective sound source location be always identified without the correct propagation model?

- Consider an idealised source in the form of a ring of point quadrupole sources put in the jet (its location varies in the jet)

$$R_{ijkl}(\mathbf{y}, Д\mathbf{y}, \omega) = \delta(y_1 - x_s)\delta(y_3 - r_s)\delta(\eta_1 - x_s)\delta(\eta_3 - r_s)\alpha_{ijkl},$$

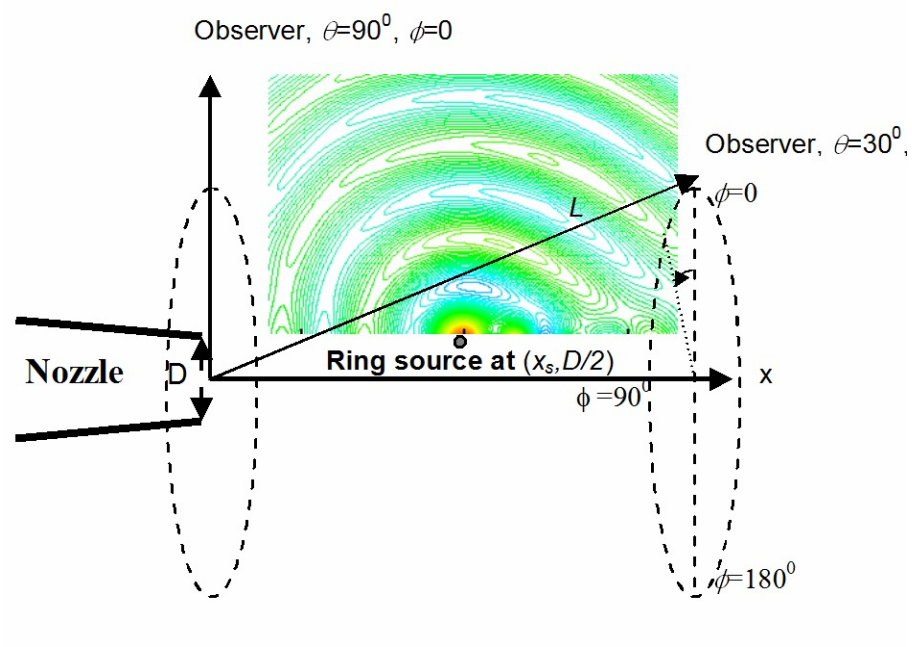

Compare the full propagation model spectra (F) with an approximate meanflow model (A)

Results

- For 90^0 the F and A spectra collapse for frequencies 1<St<2; the same source locations are predicted
- For 30^0 the F and A are different; this leads a 4Dj apparent shift in the source location

F, xs/D=7

A, xs/D=3

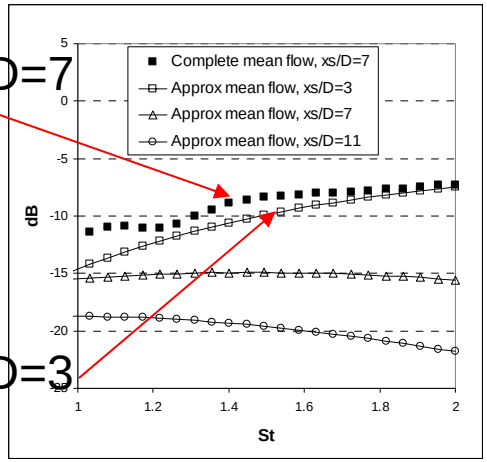

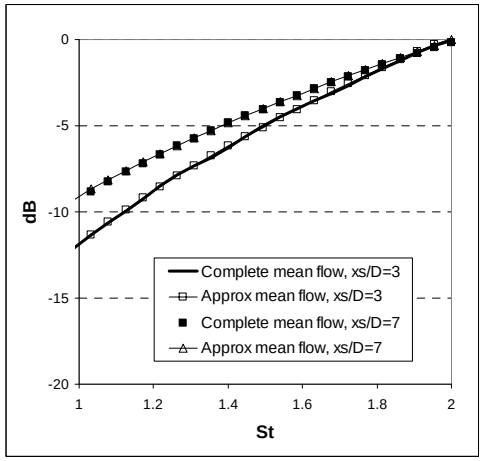

Results

- For 90^0 the F and A spectra collapse for frequencies 1<St<2; the same source locations are predicted
- For 30^0 the F and A are different; this leads a 4Dj apparent shift in the source location

F, xs/D=7

A, xs/D=3

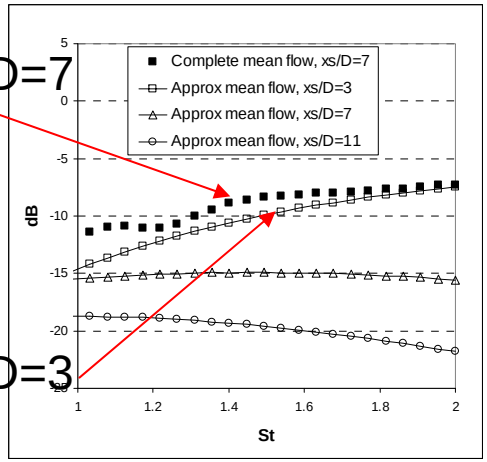

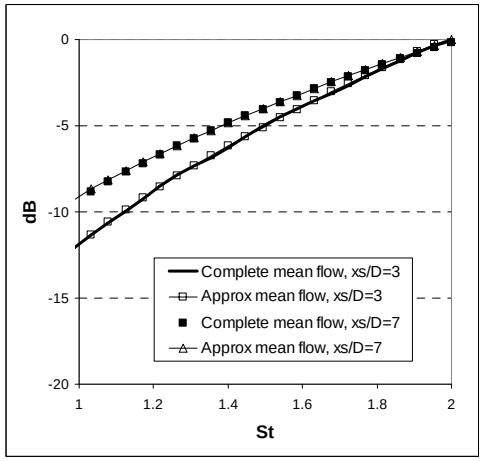

??

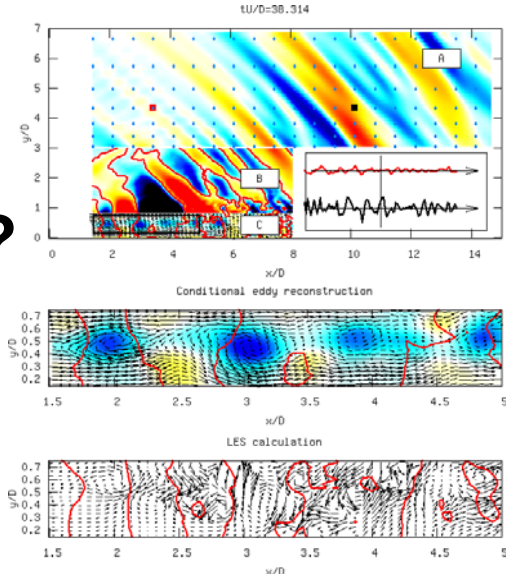

Kerherve et al, AIAA 2010-3965

- Promote the use of the full LEE solution for determining the locations of effective structures in the jet that correlate with the far field

Advantages: numerical beamforming

- Our model allows us to identify the location of the effective sources of far-field sound in the jet that includes the full propagation effects

30^0 to the jet **St=0.2** **St=1** **St=2**

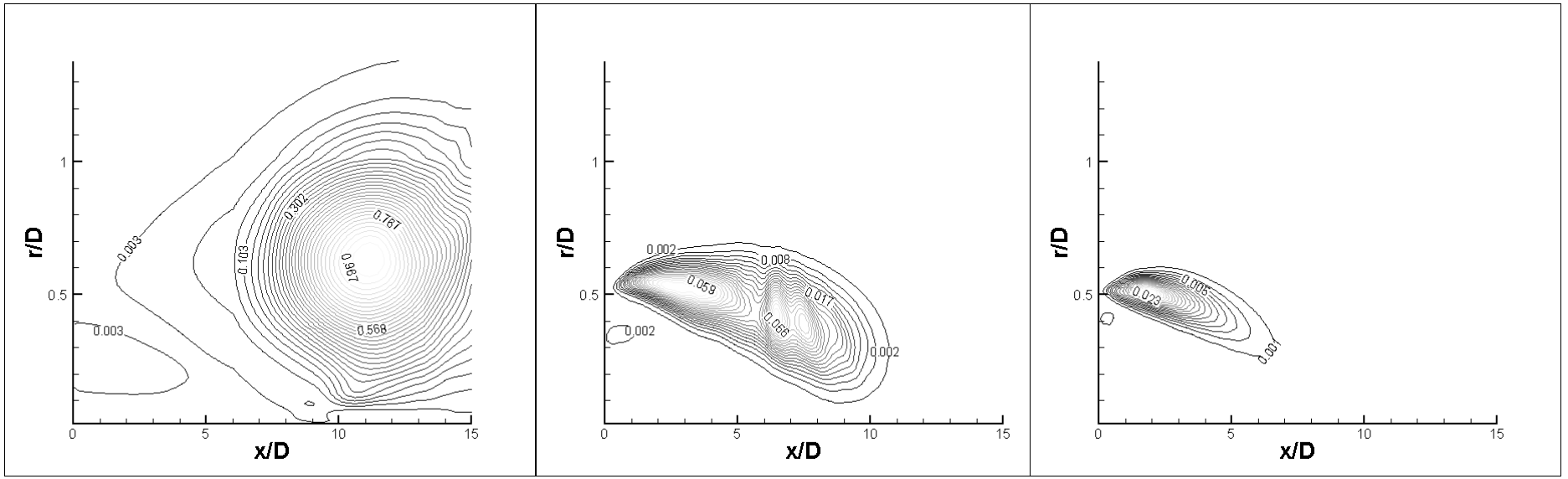

Contours of contributions to acoustic pressure power spectral density, i.e. the inner convolution product of the propagation operator based on the Green function and the source function based on the Gaussian source description informed by LES, normalised by the peak sound value

But certain open questions remain

- Intermittency effects for laminar/transitional jets
- LES near field data from C.Bogey for
  - conditions: isothermal M=0.9, $Re=10^5$
  - axi-symmetric nozzle of diameter D_j with a blunt lip
  - thin shear layer
  - 3 cases: (1) no forcing, (2) 250 Pa forcing, (3) 2000 Pa forcing
- Attempting to do the same acoustic postprocessing as for the previous JEAN and SHJAR jet cases

But certain open questions remain

- Intermittency effects for laminar/transitional jets
- LES near field data from C.Bogey for
  - conditions: isothermal M=0.9, Re=10^5
  - axi-symmetric nozzle of diameter D_j with a blunt lip
  - thin shear layer
  - 3 cases: (1) no forcing, (2) 250 Pa forcing, (3) 2000 Pa forcing
- Attempting to do the same acoustic postprocessing as for the previous JEAN and SHJAR jet cases
- Autocorrelation amplitudes show the effect of the jet forcing

Postprocessed LES data from C.Bogey (C.Hale)

No forcing

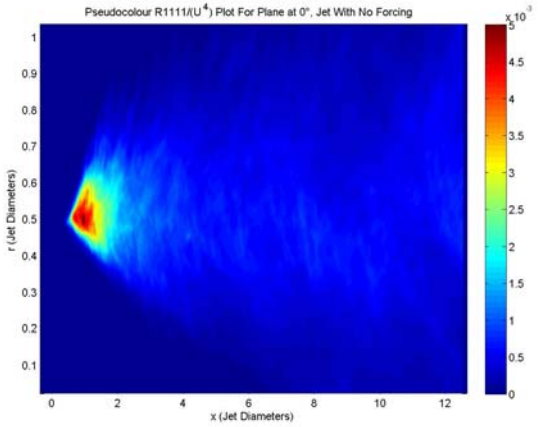

With 2000 Pa forcing

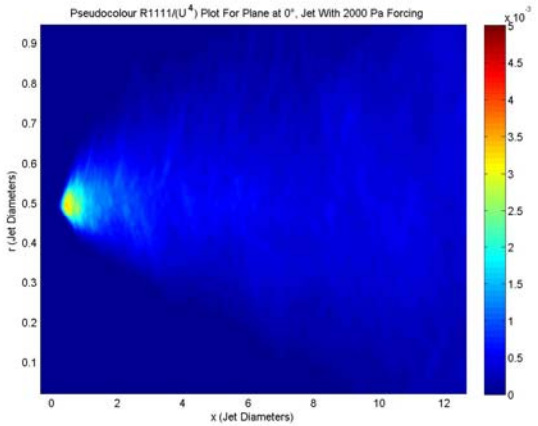

But certain open questions remain

- Intermittency effects for laminar/transitional jets
- LES near field data from C.Bogey for
  - conditions: isothermal M=0.9, Re=10^5
  - axi-symmetric nozzle of diameter D_j with a blunt lip
  - thin shear layer
  - 3 cases: (1) no forcing, (2) 250 Pa forcing, (3) 2000 Pa forcing
- Attempting to do the same acoustic postprocessing as for the previous JEAN and SHJAR jet cases
- But … the Gaussian fits don't work everywhere in the jet

Postprocessed LES data from C.Bogey (C.Hale)

Fit error

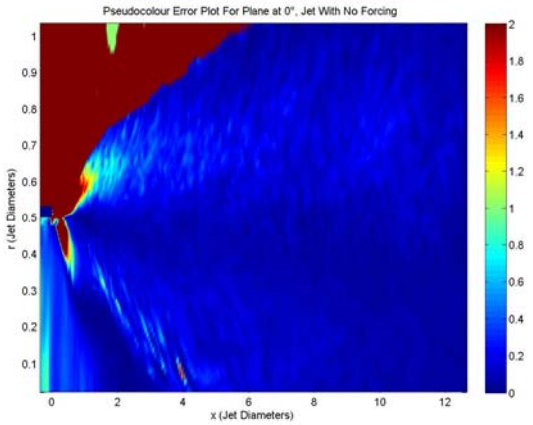

Map of correlation length scales

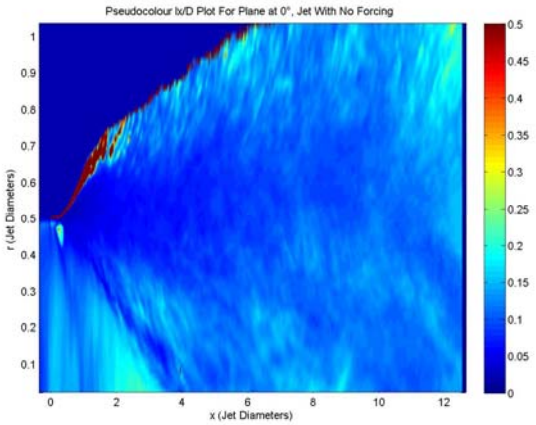

Certain open questions remain

- Preliminary sound prediction results for 90^0 to the jet (the complete Linearised Euler model results for all angles are underway)

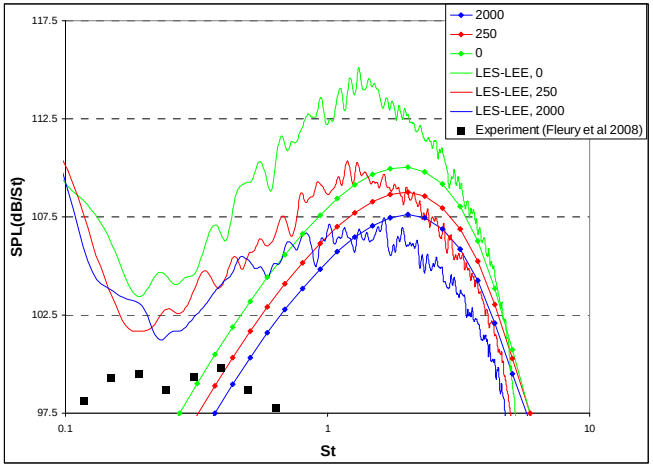

- Captures the trends but the long frequencies appear to be missing from the source model
- Q: How do you define the average when intermittent events are present?
- Suggests a different way of postprocessing for different parts of the jet, e.g., conditional filtering (under way)

Conclusions

- Hybrid methods can be used for the identification of jet noise sources
- Propagation/sound interference effects are important
- The generalised Goldstein-type approach based on LEE has promise: it is tunable parameter free and has correct propagation, possible merger with RANS (still no tuning!)
- Transitional jets model has been semi-successful, more work to be done (e.g., conditional source filtering)

The ultimate goal: aircraft noise reduction

Must consider jet engine installation effects: e.g., Flap Jet Interaction (FJI) noise

- FJI: may have a strong adverse effect at takeoff, and the mechanism is NOT dipole! Has **both** tonal and broadband components.
- Mengle et al, AIAA-2007-3666 showed that the effects of the flaperon trailing edge introduced by the analogy with airfoil self-noise didn't yield any notable noise decrease and, in some cases, even lead to a noise increase.
- Flap noise test cases: a typical wing-flap configuration: the visualisations of the acoustic field for the side-line location of the phased microphone array at peak sound frequency for approach (a) and takeoff (b) conditions.

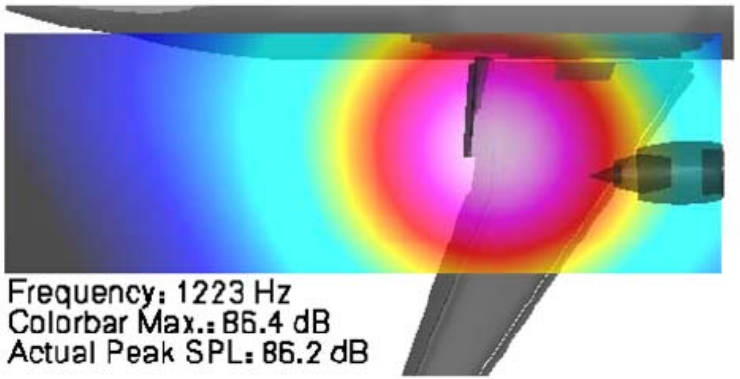

(a)

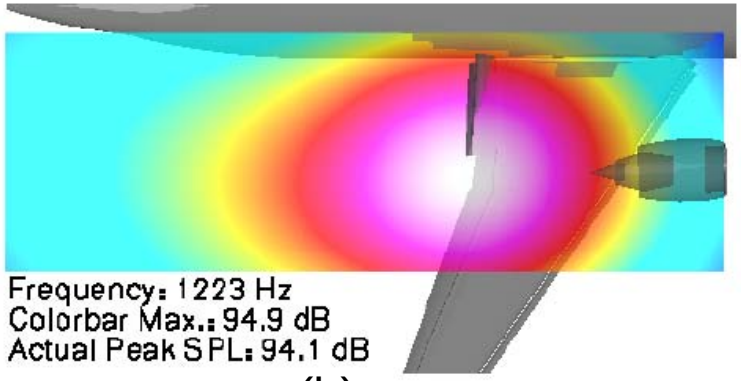

(b)

Combining the broadband and tonal noise effects within a generalised prediction method?

- Idea: “Porous Goldstein analogy” by analogy with the classical FW-H,
- The FW-H trick:

Introduce a Heaviside step-function $H(f)$ that corresponds to the control surface location (*f*=0)

$$\frac{\partial}{\partial t}\left(H(f)\cdot\rho'\right)+\frac{\partial}{\partial x_i}\left(H(f)\cdot\rho v_i\right)=\left(\rho_0 v_n+\rho' v_n\right)\delta(f)\left|\nabla_x f\right|,$$

$$\frac{\partial}{\partial t}\left(H(f)\cdot\rho v_i\right)+\frac{\partial}{\partial x_j}\left(H(f)\cdot\left(\rho v_i v_j+p_{ij}\right)\right)=\left(p_{ij}n_j+\rho v_i v_n\right)\delta(f)\left|\nabla_x f\right|.$$

In the FW-H method these equations are rearranged to a heterogeneous linear wave equation form (the Lighthill equation) with respect to the generalised variable

$p \leftrightarrow H(f)\cdot p$ (outside the control surface these are the same)

and solved with a free-space Green’s function method to obtain the pressure signal at the far field. This usually neglects the outside quadrupole term.

“Porous Goldstein”, idea

Do the FW-H trick for the Goldstein set of equations, then

$$\mathbf{L}\cdot\left(H(f)\mathbf{V}^{(n)}\right)=Sources(\mathbf{y})+S(\mathbf{y}),\ p(\mathbf{x})=\int_{R^3(A)}G(\mathbf{x}|\mathbf{y})Sources(\mathbf{y})dy+\int_{R^2(B)}G(\mathbf{x}|\mathbf{y})S(\mathbf{y})dy,$$

$$H(f)\mathbf{V}^{(n)T}\equiv(H(f)\rho,H(f)u,H(f)v,H(f)w,H(f)p),\mathbf{x}=farfield,\mathbf{y}=nearfield$$

$$S_0=\left(u_n+\rho'\tilde{v}_n\right)\delta(f)\left|\nabla_x f\right|$$

$$S_i=\left(p_{ij}n_j+u_i\tilde{v}_n\right)\delta(f)\left|\nabla_x f\right|\quad i=1,..3.$$

$$S_4=\left(p'\tilde{v}_n/(\gamma-1)+u_n\tilde{h}\right)\delta(f)\left|\nabla_x f\right|.$$

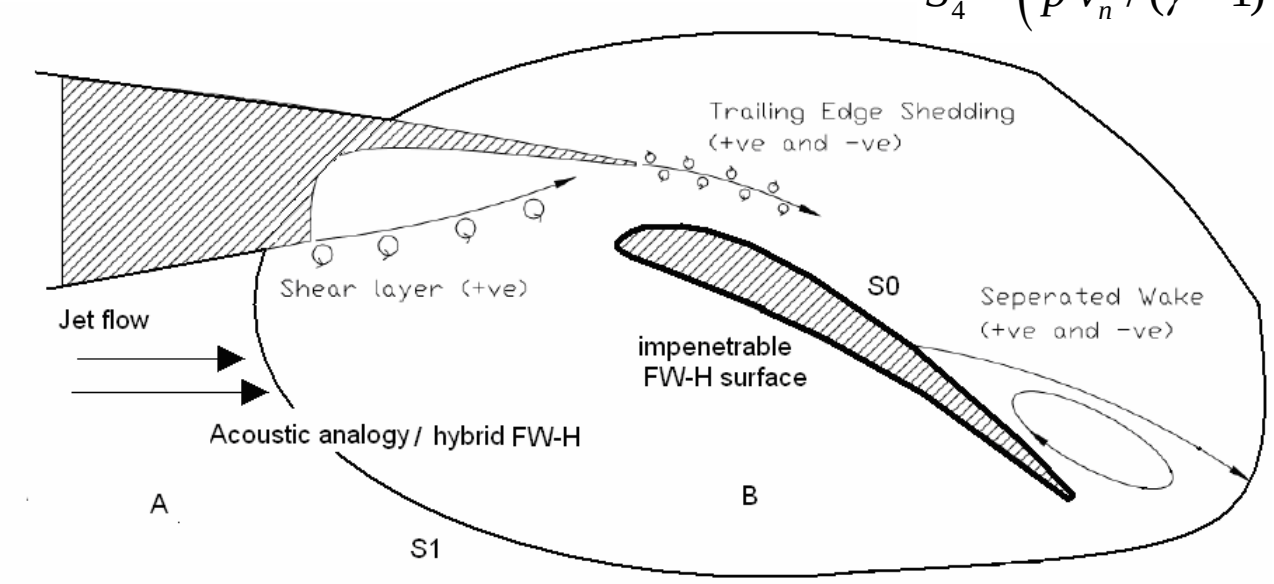

“Porous Goldstein”, advantages:

- Consistent source decomposition for capturing the tonal and broadband noise sources based on the representation theorem
- Can be based on the first principle tools (e.g., LES); but allows studying the opportunities for semi-empirical methods (e.g.,RANS)
- Full propagation modelling using the linearised Euler

Flap Noise Project

Supported by the Engineering and Physical Sciences Research Council (UK)

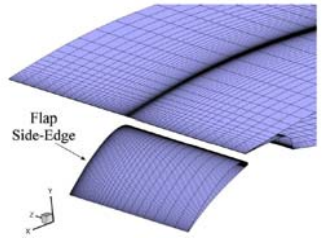

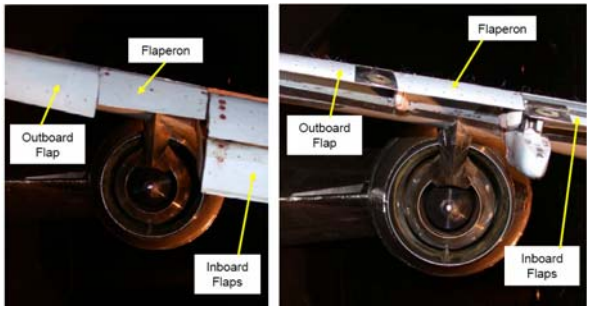

- A new 30 months project to start in 2011
- Concentrate on Flap noise + Flap jet interaction noise
- New “porous Goldstein” formulation to be developed and tested for several model configurations including passive control options for flap edges.
- CFD source modelling: LES, ILES, HYDRA (Rolls-Royce), CABARET
- Computing (HECToR UK Cray Supercomputer)
- People: SK, Vasily Goloviznin (NSI Moscow), Paul Tucker (Engineering, Cambridge), Nigel Peak (Applied Mathematics, Cambridge), postdoc (to be appointed)
- Industrial contacts: Jerome Huber (Airbus), Paul Strange (Rolls-Royce)